Electrochimica Acta 110 (2013) 418–427

Contents lists available at ScienceDirect

Electrochimica Acta

journal homepage: www.elsevier.com/locate/electacta

Ion transfer dynamics of poly(3,4-ethylenedioxythiophene) films in deep eutectic solvents

A. Robert Hillman[a,*], Karl S. Ryder[a], Virginia C. Ferreira[a], Christopher J. Zaleski[a], Eric Vieil[b]

[a] Department of Chemistry, University of Leicester, Leicester LE1 7RH, UK
[b] Université Grenoble 1, F-38402 Saint Martin d'Hères, France

ARTICLE INFO

Article history:
Received 22 February 2013
Received in revised form 13 July 2013
Accepted 15 July 2013
Available online 29 July 2013

Keywords:
Conducting polymer
PEDOT
Deep eutectic solvent
QCM
Probe beam deflection
Ion transfer

ABSTRACT

Mechanistic studies are reported for redox switching (doping/undoping) of Au-supported poly(3,4-ethylenedioxythiophene) (PEDOT) films exposed to $LiClO_4/CH_3CN$ (a conventional electrolyte based on a molecular solvent) and to Ethaline and Propaline (two choline chloride-based deep eutectic solvent (DES) media). A combination of electrochemical, acoustic (quartz crystal microbalance, QCM) and optical (probe beam deflection, PBD) methods was used to monitor the exchange of mobile species between the film and the bathing electrolyte. Qualitatively, film responses to a potentiodynamic control function showed that the redox switching mechanisms are quite different in all three media. When exposed to acetonitrile, *anion* transfer is dominant, with some accompanying solvent transfer but negligible cation transfer; application of the convolution protocol allowed these transfers to be quantified. Analogous observations in the DES media could be interpreted qualitatively in terms of dominant *cation* transfer, but the convolution protocol could not be used to quantify the contributions of individual species; in these viscous media, this is a consequence of the long transit times from the film/solution interface to the optical detection zone. Chronoamperometric experiments, in which the measurement time was an order of magnitude (or more) longer permitted the diffusional processes driven by the polymer/DES interfacial population changes to reach the optical detection zone.

1. Introduction

Quite generally, rapid switching – manifested in terms of (dis)charge rate, optical response time or sensor response time, according to the application – is central to the performance of devices using electroactive conducting polymer films as the active material. Since the rate of electron transport is relatively rapid, changes in charge state are invariably limited by the rate(s) of ion transfer(s) required to maintain electroneutrality ("doping" in the parlance of the field). Commonly, one chooses to use an electrolyte of high ionic strength in order to maximise the availability of dopant ions, but for conventional electrolytes based on molecular solvents (even as polar as water or acetonitrile) the ionic concentration is seldom much more than 1 M. Encouraged by other practical reasons – including wide potential window, low volatility, low toxicity, environmental acceptability and cost – we have been investigating the use of room temperature ionic liquids as electrolytic media. An additional attraction of these media, which we seek to exploit here, is that the ion concentration is extremely high: there is no "solvent" in the conventional sense of the term and the fluid is entirely ionic. Not only does this hold the promise of practically limitless availability of ions from the liquid phase, but also even modest partition of electrolyte (equivalent amounts of anions and cations) into the film will provide high conductivity to accelerate switching of films from the undoped (neutral) state. The purpose of the present study is to explore these very attractive technological possibilities and the interesting fundamental questions presented by the absence of molecular solvent, which is generally associated with such phenomena as osmosis and plasticisation-driven viscoelasticity.

The electronic and optical properties of conducting polymers make them attractive materials for diverse (electro)chemical applications, as reviewed elsewhere [1,2]. The structural feature upon which these applications rely is a conjugated π–electron system able to act as a source/sink for electronic charge, such that oxidation (p-doping) or reduction (n-doping) results in partially filled bands containing highly mobile charge carriers. Pyrrole, thiophene and aniline and a number of their substituted derivatives can be polymerised to produce materials that fulfil these criteria. When polymerisation is carried out electrochemically, the resultant

* Corresponding author. Tel.: +44 116 252 2144; fax: +44 116 252 5227.
E-mail address: arh7@le.ac.uk (A.R. Hillman).

0013-4686/$ – see front matter © 2013 Elsevier Ltd. All rights reserved.
http://dx.doi.org/10.1016/j.electacta.2013.07.120

polymers are deposited on the electrode surface as thin films that can subsequently (in monomer-free solution) be reversibly doped and undoped at a rate and to an extent that can be controlled by the applied potential [1,2].

In this study we focus on poly(3,4-ethylenedioxythiophene) (PEDOT), a polythiophene derivative whose substitution pattern results in facile polymerisation, enhanced chemical/environmental stability, excellent longevity under redox cycling, convenient redox energetics and a p-doped state with conductivity up to 500 S cm^{-1} [1,2]. These attributes have lead to the use of PEDOT in charge storage devices [3], micro-electrochemical [4] and organic thin film [5] transistors, antistatic coatings [6], photovoltaic energy conversion [7], electrochromic and optical display devices [8,9], corrosion protection coatings [10], drug delivery [11], biosensors [12], electrocatalysis [13], memory devices [14], fluid handling devices [15] and mechanical actuators [16].

Performance optimisation in the above applications has motivated a number of mechanistic studies of the (un)doping of PEDOT [17–24] and other conducting polymers [25–28]. Nevertheless, the details of the underlying redox-driven ion and solvent exchange processes – in terms of both the overall film population changes of these mobile species and the rates at which they occur – are not fully understood. One reason for this is that the rates of the competing ion transfers, *e.g.* anion entry *vs* cation ejection during p-doping, depend significantly on a number of factors: on the *ions* themselves (*via* size and geometry); on the *solvent* (which may be coordinated to the ions and/or swell the polymer); and on the *polymer* morphology (which will depend on the film deposition conditions and subsequently film redox history) [29,30]. Significantly, the polymer is not a static medium, but has a rich dynamics commonly manifested *via* viscoelastic phenomena [31,32]. All these factors complicate not only the analysis of individual studies but also comparison with nominally identical studies by different researchers.

PEDOT is one of the most intensely studied of all the substituted heterocyclic conducting polymer systems. This is partly because of its chemical and electrochemical stability, by virtue of complete substitution of the thiophene ring system, and partly because of its unusual optical and electrochromic properties [33]. In addition, PEDOT is easily blended with polyanionic materials, such as polystyrenesulfonate, in order to produce solution processable materials. Much of this research has been focussed on potential applications of PEDOT films in functional materials; this diverse range of applications has been reviewed elsewhere [34]. More recently the studies of PEDOT and substituted variants have focussed on particular applications and challenges. These include, for example roll-to-roll manufacturing of printed sheet plastic electronics [35], photocatalysis [36], integrated textile heating elements as well as heat sensors [37,38], solar cell energy harvesting films [39] and ink-jet printable photovoltaics [40]. In all of these applications the key challenges associated with optimising performance focus on electron transfer, counterion transfer and polymer chain dynamics. In applications where the polymer film is in contact with a liquid/electrolyte phase, *e.g.* energy storage or sensing, it is also important to understand and quantify the influence of coupled solvent transfer. This is clearly a moot point when comparing molecular solvent systems and ionic liquids.

The majority of mechanistic studies of conducting polymer redox chemistry and of its implementation in practical devices have involved the use of electrolytes dissolved in molecular solvents, notably water and acetonitrile. More recently, the use of room temperature ionic liquids [41,42] has been explored in this context. In many instances, the motivation for using these media has been elimination of volatile, toxic or combustible solvent (for safety reasons) or the opportunity to exploit a wide potential range [43]. While these are attractive features, our motivation has centred on the goal of increasing the ion transfer rate. Since the fluid is composed entirely of ions, the availability of dopant is raised to levels that are not possible in conventional electrolyte media.

An extension of the ionic liquid concept is the formation of a deep eutectic solvent (DES) [44,45], formed by mixing a suitable combination of a solid quaternary ammonium salt (QAS) and a hydrogen bond donor (HBD). In general, the HBD forms a complex with either the cation or anion of the QAS. In the present study, the QAS is choline chloride (Ch^+Cl^-) and the HBD is either ethylene glycol (EG) or propylene glycol (PG), in each case in a 1:2 molar ratio of QAS:HBD. In these formulations (formally denoted Ethaline 200 and Propaline 200, respectively, to indicate stoichiometry, but hereafter referred to simply as Ethaline and Propaline), the HBD complexes the anion, to give a fluid that is mixture of Ch^+ cations and $[(EG)_2Cl]^-$ or $[(PG)_2Cl]^-$ anions.

A recent report [46], based on electrochemical and acoustic wave (EQCM) data, showed that the ion transfer processes accompanying PEDOT redox switching in Ethaline 200 and Propaline 200 are different to each other and to those in a conventional acetonitrile-based electrolyte. Overall, we seek an understanding of ion dynamics accompanying PEDOT (un)doping in DES media. Specifically, we wish to determine the individual contributions of anion and cation to maintenance of electroneutrality as functions of timescale and polymer charge state (doping level). Second, we wish to identify the rate limiting process; this is important both for fundamental and practical reasons. Third, simple considerations show that some mechanistic possibilities, *e.g.* cation ejection upon film oxidation, require the presence of a "reservoir" of net neutral electrolyte ("salt" in the parlance of the ion exchange literature [47,48]). We therefore wish to establish the population of the film-based reservoir able to support this process.

In a recent EQCM study [46] we showed that during the potentiodynamic oxidation (p-doping) of neutral (undoped) PEDOT exposed to $LiClO_4/CH_3CN$, to Ethaline and to Propaline, respectively, the film mass increased, decreased, and varied non-monotonically (decreased then increased). This indicated anion entry in acetonitrile (the anticipated result in a conventional electrolyte), cation ejection from a DES swollen film in Ethaline, and a mixed mechanism in Propaline. Qualitatively, these observations were compelling, but each medium presents its challenges to the EQCM. In the case of a conventional electrolyte, there are three mobile species (anion, cation and solvent) so, strictly, measurement of mass (*via* frequency) and charge is an under-determined situation and one is obliged to make the approximation of permselectivity at modest electrolyte concentrations [47,48]. In DES media this chemical problem does not exist, since there is no "solvent", but the high fluid viscosity makes the acoustic measurement physically much more difficult, since the resonance is highly damped and less precisely defined, even in the absence of film viscoelastic phenomena [46].

Previously, we demonstrated the power of the combined EQCM/probe beam deflection (PBD) technique [49,50] in situations where complex mobile species transfers occur at electroactive film/electrolyte interfaces. The PBD technique (sometimes referred to as the "mirage effect") is a contactless optical method in which deflection of a light beam (generally from a small laser) passing close and parallel to the electrode surface is used as a measure of interfacial concentration gradients [51]. In the present context, these concentration gradients are generated by redox-driven exchange of species between an electroactive film and the electrolyte to which it is exposed. From a mathematical perspective, the problem is now uniquely defined: three measurands (charge (Q), mass change (Δm) and optical deflection (θ)) permit unambiguous determination of the three mobile species population changes. More subtly, the acoustic and optical techniques are complementary in two respects. First, one (QCM) probes the "dry" side of the interface and the other (PBD) probes the "wet" side of the

polymer/electrolyte interface. Second, electrical, acoustic and optical sensitivity factors for a given species are quite different, so different species are more or less readily seen by the different techniques; the gravimetric near "invisibility" of the proton and the absence of a charge response for solvent transfer are extreme examples. These collective attributes provide a compelling argument for application of the EQCM/PBD technique to PEDOT/DES systems.

There is both instrumental (technique-oriented) and chemical novelty to this work. In the former instance, we are not aware of previous application of the PBD technique in DES media, and certainly not in conjunction with the EQCM. As revealed below, this provides interesting and non-trivial challenges, whose solution opens the door to wider application of the technique. In the latter instance, the fundamentally different behaviour of PEDOT films when presented with practically unlimited ion sources is novel and has practical significance for applications, such as energy storage, that require high current and thence high ion availability.

2. Experimental

2.1. Reagents

Choline chloride (ChCl), ethylene glycol (EG), propylene glycol (PG), acetonitrile, lithium perchlorate and 3,4-ethylenedioxythiophene (EDOT) (Sigma–Aldrich) were used as received. Ethaline 200 (ChCl:EG = 1:2 mole ratio) and Propaline 200 (ChCl:PG = 1:2 mole ratio) were prepared as previously described [46] and stored at 50 °C prior to use.

2.2. Instrumentation

The electrochemical cell was a standard three-electrode configuration within a 42 mm × 42 mm × 30 mm optical glass cuvette (Hellma) [49,50]. The working electrode was one of the Au electrodes (diameter 5.0 mm, electroactive area 0.23 cm^2, piezoelectric area 0.21 cm^2) of a 10 MHz AT-cut quartz resonator (ICM Manufacturing, Oklahoma City, USA). The crystal was mounted on the end of a 55 mm glass tube (o.d. 13 mm) such that only one face was exposed to solution. The counter electrode was an Ir-coated Ti mesh. An Ag/AgCl wire exposed to the chloride media was used as a reference electrode; stability and calibration of the reference potential in choline chloride based eutectics have been discussed elsewhere [53]. Briefly, the chloride-rich DES results in a stable reference potential that can be calibrated by separate measurements of the redox behaviour of a stable, reversible ("model") redox couple. In this instance, slow scan (ν = 5–10 mV s^{-1}) voltammetric experiments using 50 mM $Fe(CN)_6^{3-}/Fe(CN)_6^{4-}$ showed the E^0 of this reversible redox couple was found to be 0.227 V in Ethaline 200 and 0.185 V in Propaline 200. The three electrodes were secured to the quartz cell by a Teflon lid.

The probe deflection system consisted of a 4 mW He–Ne laser (λ = 632.8 nm, Uniphase model 1122) with a 0.63 mm beam diameter. The beam was focussed to a diameter of ~80 μm by a 62.9 mm plano-convex lens. The beam was set parallel to the working electrode giving an interaction path of 5 mm. The electrochemical cell was supported in a cradle with a three dimensional translation table allowing transverse, vertical and rotational movements to adjust the distance, alignment and parallelism between the working electrode and probe laser beam. The optical detection was achieved with a dual (silicon based) photodiode (Optilas model 1243 bi-cell, 6.25 mm^2 active area). The detector was set 185 mm from the electrochemical cell, resulting in a position sensitivity of 0.44 μrad/mV. It was coupled to a home-built position sensing circuit which consisted of a photodiode, single axis position sensing amplifier connected to a 1:1 gain offsetting amplifier and a home built voltmeter. The position sensing detector converted the optical deflection signal into a DC current which was simultaneously recorded by a potentiostat (*via* an analogue input) and monitored on a digital oscilloscope (Gould, 20 MHz digital storage type 1425).

The entire PBD-EQCM instrument was mounted on a 100 mm steel core breadboard which was isolated from the floor by eight home built vibration dampeners. The electrochemical, gravimetric and optical signals were simultaneously recorded by a Gamry 600 potentiostat integrated with a Gamry eQCM 10M system which was coupled to home-built optical deflection apparatus described elsewhere [49,50].

For a concentration-dependent refractive index, the laser beam deflection is described by:

$$\theta(x,t) = \left(\left(\frac{l}{n}\frac{\partial n}{\partial c}\right)\left(\frac{\partial c(x,t)}{\partial x}\right)\right) \quad (1)$$

where θ denotes laser beam deviation, l is the interaction length, and $\partial n/\partial c$ represents the relationship between the species concentration c and the refractive index n [49–51]. The laser beam is deflected towards the region of higher refractive index. Thus, a positive deflection indicated the concentration increasing in the vicinity of the electrode while a negative deflection indicated a decrease of the concentration in the vicinity of the electrode.

Film morphology was observed by atomic force microscopy (AFM) (Digital Instruments, Dimension TM 3100 microscope). Measurements were made *ex situ* in tapping mode.

2.3. Procedures

PEDOT films were deposited potentiostatically (1.2 V for 30 s, with $Q_{dep.} \approx$ 26 mC) at room temperature (20 ± 2 °C) using the procedure reported previously [46], from a 0.05 M EDOT monomer solution in 0.1 M $LiClO_4$ in CH_3CN. After deposition the films were rinsed with CH_3CN, dried and immersed in the characterisation solution where they were allowed to stabilise before measurements. While minor variations in absolute responses for nominally identical films were obtained, the magnitudes of the responses scale with film charge; consideration of molar mass changes accomplishes this normalisation naturally. In each instance, individual film charge is given in the associated figure legend. In order to permit comparison of data acquired under different conditions without fear of "drift" in film properties, two precautions were taken. First, the deposition and handling procedure was found to give films with electrochemical and gravimetric signatures to repetitive measurements that did not vary by more than 5% or better over 50 redox cycles. Second, we generally conducted "bracketed" experiments, in which a given measurement was conducted at the outset and at the end of a set of diverse measurements: consistent responses eliminate the possibility of irreversible film ageing as a contributing factor. Under conditions where dissipation in the film was not significant, a full spectral fit was made to the acoustic resonator response to yield the resonant frequency, which was then interpreted gravimetrically using the Sauerbrey equation [54], as described previously [46].

3. Results and discussion

3.1. Film responses to potentiodynamic control function

3.1.1. Raw data and qualitative interpretation

As a direct extension to our previous EQCM study [46], the initial aspiration was simply to add in the PBD measurement and, by combining all three responses (i, Δm, θ), thereby resolve the individual mobile species transfers unambiguously. Representative data for such a set of experiments are shown in Fig. 1 for a film

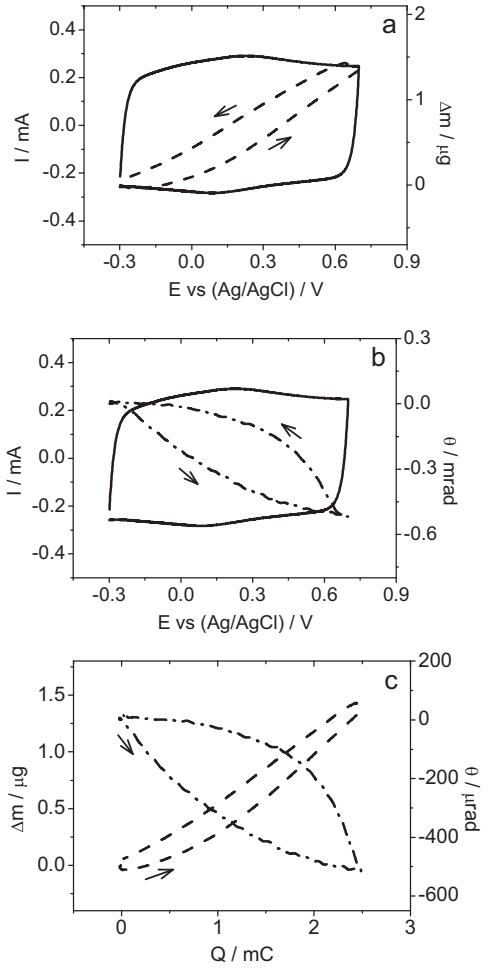

Fig. 1. Current (i; full line), mass (Δm; dashed line) and optical deflection (θ; dot-dashed line) responses to a potentiodynamic experiment (scan rate, $v = 100\,\text{mV s}^{-1}$) for a PEDOT film ($Q_{dep} = 25.95\,\text{mC}$; dry thickness $h_f^0 = 0.62\,\mu\text{m}$ exposed to 0.1 M $LiClO_4/CH_3CN$. Panel a: i *vs* E and Δm *vs* E; panel b: i *vs* E and θ *vs* E; panel c: Δm *vs* Q and θ *vs* Q, where Q is the charge (from integration of i, set to zero at the start of the cycle, $E = -0.3\,\text{V}$). Arrows indicate scan directionality.

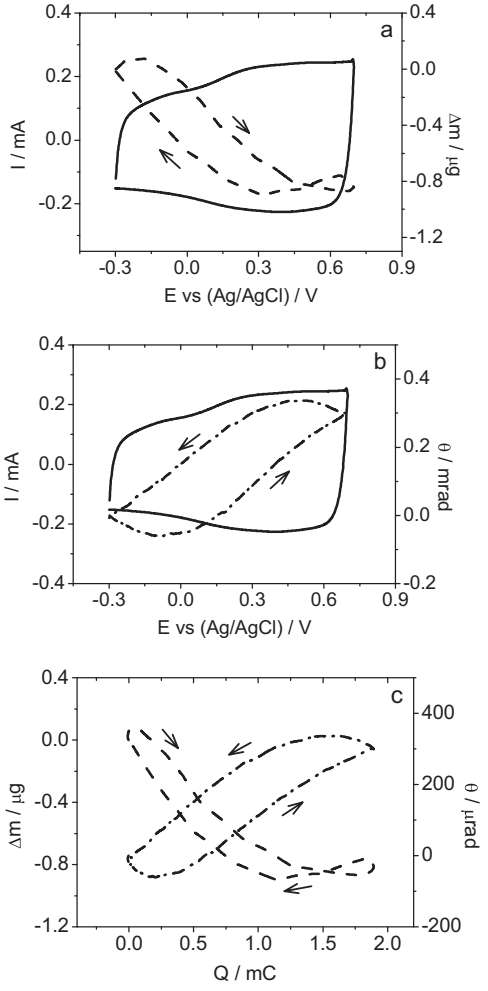

Fig. 2. Current (i; full line), mass (Δm; dashed line) and optical deflection (θ; dot-dashed line) responses to a potentiodynamic experiment (scan rate, $v = 100\,\text{mV s}^{-1}$) for a PEDOT film (that of Fig. 1) exposed to Ethaline. Panel a: i *vs* E and Δm *vs* E; panel b: i *vs* E and θ *vs* E; panel c: Δm *vs* Q and θ *vs* Q, where Q is the charge (from integration of i, set to zero at the start of the cycle, $E = -0.3\,\text{V}$). Arrows indicate scan directionality.

exposed to a molecular solvent medium (0.1 M $LiClO_4/CH_3CN$) and in Figs. 2 and 3 for a film exposed to the two DES media, Ethaline and Propaline, respectively.

Before discussing the significance of the acoustic (QCM) response, it is necessary to distinguish the relative contributions of the film and the ambient fluid to acoustic loss (damping). The situation is somewhat different for films exposed to DES media (such as Ethaline and Propaline) and to conventional molecular solvents (such as acetonitrile). Acetonitrile has relatively low viscosity, so polymer viscoelastic phenomena commonly have a dramatic effect on acoustic resonator response, particularly for highly solvated films. Conversely, DES media have relatively high viscosity, so their presence commonly dominates viscous loss. The experimental data are consistent with these general statements. Specifically, immersion into DES of a bare crystal (prior to polymer deposition) from air results in a resonant admittance decrease from 20 mS (in air) to 0.58 mS in Ethaline and 0.63 mS in Propaline. When the resonator is polymer-coated, the resonant admittance is 0.51 mS in both Ethaline and Propaline media. It is clear that the dominant factor in viscous loss is the electrolyte, not the polymer film; we therefore interpreted the redox-driven resonant frequency changes gravimetrically.

Qualitatively, the responses are readily comprehensible. In acetonitrile, the film mass increases upon PEDOT oxidation (p-doping) and the accompanying optical deflections are negative, indicating a beam deflection away from the electrode. Both these are consistent with interfacial depletion of the solution of anions, which enter the film as dopant species. There is hysteresis in the optical and gravimetric signals, whether plotted as functions of potential or charge. In the case of their dependence on applied potential, this signals kinetic effects in terms of the mass response and kinetic and/or diffusional effects (see below) in terms of the optical response. Since the hysteresis is still present when considered as a function of injected charge, arguments based on electroneutrality and Faraday's law mean that there must be more than one species transferred, *i.e.* anion and (at least) solvent.

In the two DES media, the film mass *decreases* upon PEDOT oxidation (p-doping). In Ethaline the accompanying optical deflections are positive, indicating a beam deflection towards the electrode, and in Propaline the optical deflection is non-monotonic, suggesting a change in mechanism. These observations are consistent with a cation transfer-based mechanism in Ethaline and a two-stage mechanism in Propaline. As in acetonitrile, there is hysteresis in the responses, although of a somewhat more complex nature here.

The acetonitrile data are entirely consistent with the widely accepted facts that PEDOT oxidation results in anion doping and a solvation state change [21,22]. We make no novel claims here,

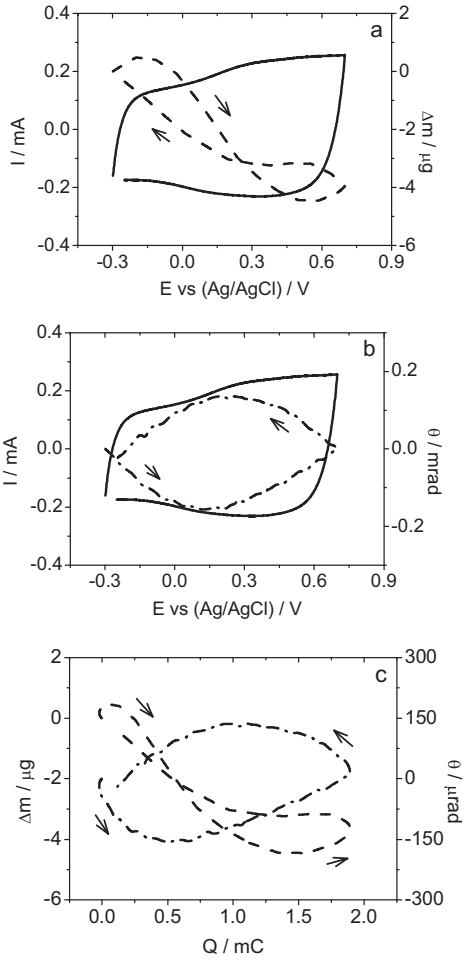

Fig. 3. Current (i; full line), mass (Δm; dashed line) and optical deflection (θ; dot-dashed line) responses to a potentiodynamic experiment (scan rate, $\nu = 100\,\mathrm{mV\,s^{-1}}$) for a PEDOT film (that of Fig. 1) exposed to Propaline. Panel a: i *vs* E and Δm *vs* E; panel b: i *vs* E and θ *vs* E; panel c: Δm *vs* Q and θ *vs* Q, where Q is the charge (from integration of i, set to zero at the start of the cycle, $E = -0.3\,\mathrm{V}$). Arrows indicate scan directionality.

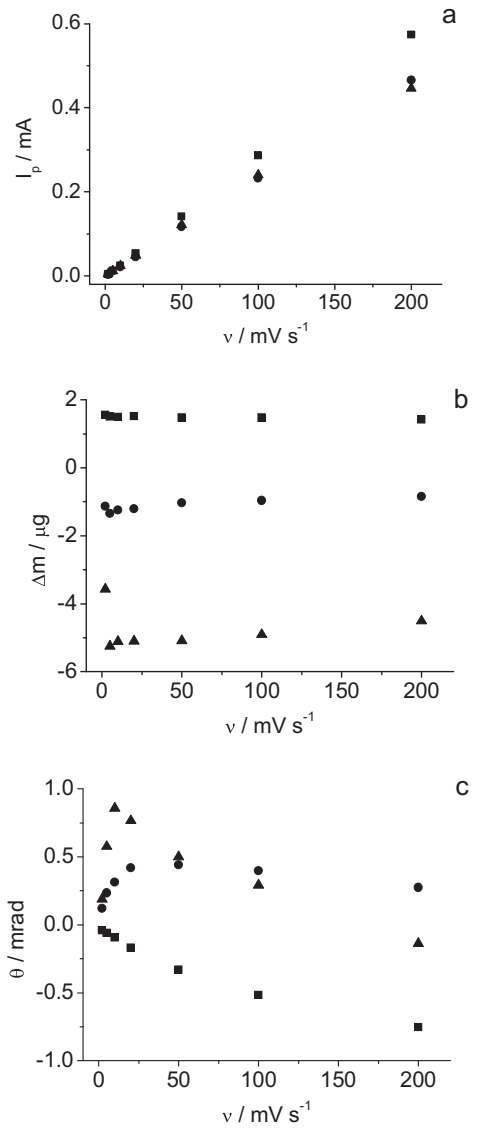

Fig. 4. Magnitudes of PEDOT film (that of Figs. 1–3) responses to potentiodynamic experiments as a function of potential scan rate. Panel a: current (i); panel b: mass change (Δm); panel c: optical deflection (θ). Media to which film was exposed were: 0.1 M $LiClO_4/CH_3CN$ (■), Ethaline (●) and Propaline (▲).

but simply demonstrate that the PEDOT films produced are typical of those studied elsewhere and can be used to provide the "baseline" from which the DES studies are developed. In the latter instance, the observations themselves are novel and the combination of techniques is novel in the context of ionic liquids as a class of materials.

3.1.2. Quantitative interpretation

Moving to the first stage of a quantitative interpretation, we consider the magnitudes of the responses: in the case of current we consider peak current (although we note that the responses are rather "flat" as a function of potential); in the case of mass change and optical deflection, we consider the largest excursions (since the responses are non-monotonic in the DES media under certain conditions). These parameters were determined as a function of scan rate by extraction from a series of experiments analogous to those of Figs. 1–3 in the range $2 \leq \nu/\mathrm{mV\,s^{-1}} \leq 200$. The outcomes are plotted in Fig. 4.

Notwithstanding some experimental scatter in the data, the peak current values are broadly linear with scan rate and, perhaps surprisingly, are not very different in the three different media. The message here is that, although charge compensation may be accomplished by different ion transfers, the film redox conversion is complete, *i.e.* electron transfer to/from all redox sites occurs throughout this range of timescales. However, the very different natures of the mass and optical deflection responses signal that the mechanisms by which film redox conversion occurs are quite different. This sets the central question of the study: what are those mechanisms and are the differences between the molecular solvent and the DES's predominantly associated with *film* composition and properties or *solution* behaviour *per se*?

We now turn to the mass excursions, bearing in mind that these represent (integrated) population changes, in contrast to the differential (flux-based) responses represented by the current and optical deflection. The qualitative distinction between exposure to the molecular solvent (mass increase upon film oxidation) and DES (predominantly mass decrease upon film oxidation) has already been noted (see the different signs for the data in Fig. 4b). Quantitatively, the magnitude of the overall mass change in each electrolyte is essentially independent of scan rate (timescale). The implication here is that any slower (non-field driven) net-neutral species transfers (molecular solvent or charge balanced – though not necessarily paired – ions) are completed. In the case of exposure to acetonitrile, the *overall* redox-driven film mass change is

less than that predicted by Faraday's law for anion transfer alone. This is a consequence of the anion and solvent transfers occurring in opposite directions; this type of compensatory motion is a common occurrence for electroactive polymer film redox switching in conventional electrolytes. The data in the DES media are interesting in that, despite the fact that cation transfer is dominant and the same in both media (choline), the magnitudes of the mass changes are quite different. The clear implication here is that the contributions of the "other" process(es) – $[(EG)_2Cl]^-$ or $[(PG)_2Cl]^-$ anions and/or charge-balanced amounts of cations and anions (where there is no implication made regarding ion-pairing) – are very different. From these data we conclude (see question posed above) that film compositions in the different media are quite different.

Finally, for this data set, we consider the optical deflection data. Simplistically, since this responds to a gradient of concentration (see Eq. (1)), we might expect similar behaviour to the current (another flux-based parameter). In acetonitrile, the magnitude of the optical signal excursion is non-linear with scan rate: it varies with the square root of scan rate, suggesting a diffusional process. In the DES media, the result is rather more interesting and – as will shortly become apparent – complicated. Starting from the lowest scan rate, the magnitude of the signal initially increases with scan rate; the signals are different in the two DES media, consistent with the different film-based processes deduced from the mass responses (see above). At intermediate scan rates (50 mV s^{-1} in Ethaline and 10 mV s^{-1} in Propaline), the magnitude of the optical signal excursion reaches a maximum and thereafter decreases with scan rate – dramatically so in Propaline. There are also substantive changes (data not shown here) in the shapes of the profiles and the extent of hysteresis between forward and reverse half-cycles.

The declared intent at the outset was use of the convolution process [49–51] to project the current and mass responses (acquired at the electrode surface) onto the optical response (acquired at some distance from the surface). This is the route to deconvolution of the overall responses into the constituent species contributions [49–51]. In the case of films exposed to acetonitrile, the procedure worked well; a representative example (for a scan rate, $\nu = 20$ mV s^{-1}) of the convolved current and mass responses is shown in Fig. 5. Their relatively similar form to the observed PBD response shows that, as anticipated, anion transfer dominates. More detailed analysis of the differences between the convolved current and mass and the observed optical deflection shows that there is some solvent transfer and minimal cation transfer; expressed succinctly, the film is permselective. Fig. 5 also shows a plot of $x/\sqrt{D}$ (extracted from the fitting) *vs* d, where x is the absolute value of the probe laser beam from the surface and d represents the relative position of the laser beam from the electrode surface. Experimentally, known relative variations of the electrode-beam separation (d) are straightforward to control (using stepper motors), but determination of the absolute distance (x) is not directly possible: the extrapolation shown in Fig. 5c is a device to accomplish this. The linearity of the plot is consistent with a diffusional process (from the polymer/solution interface to the laser beam). The intercept on the x-axis yields the absolute values of beam location (*ca.* 50 μm from the surface) and the slope gives a diffusion coefficient $D = 7.2 \times 10^{-6}$ cm^2 s^{-1}, consistent with expectation for a small molecule/ion in acetonitrile.

Unfortunately, this established protocol did not produce physically reasonable outcomes when applied to the majority of the data acquired in the DES media. This is a major impediment to the declared intention of making the combined EQCM/PBD methodology applicable to studies of electroactive films in DES media. In order to address this challenge we therefore require determination of the underlying physical phenomenon.

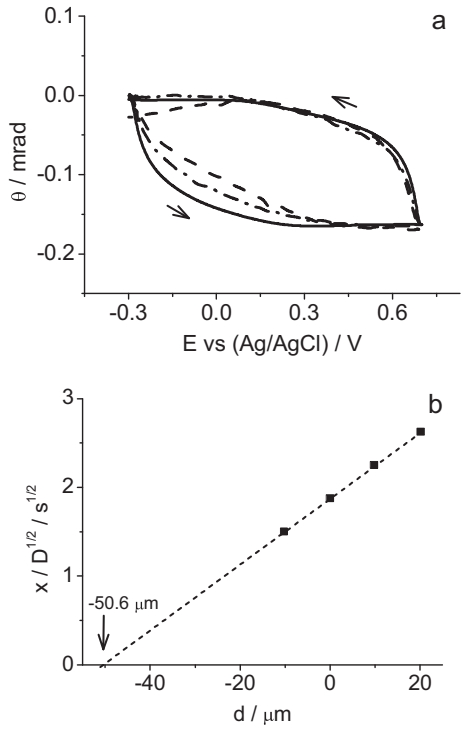

Fig. 5. Convolved data for a potentiodynamic experiment (scan rate, $\nu = 20$ mV s^{-1}) on a PEDOT film (as Fig. 1) exposed to 0.1 M $LiClO_4/CH_3CN$. (Data are from the same series of experiments that generated the data set shown in Fig. 1 and represented in Fig. 4.) Panel a: convolved current signal (full line); convolved mass change signal (dashed line); observed optical deflection signal (dot-dashed line). Arrows indicate scan directionality. Panel b: values of $(x/\sqrt{D})$ (from convolution fitting protocol) as a function of relative position (x) of probe beam.

3.1.3. Limitations of the convolution protocol under potentiodynamic conditions

Successful application of convolution to potentiodynamic PEDOT redox switching in acetonitrile media indicates that the problem does not lie with the control function *per se* or with the polymer.

In the latter instance, it is worth pointing out that AFM data give laterally averaged film thicknesses of 1.0 μm with a roughness of 99 nm (*i.e. ca.* 0.1 μm) after polymerisation; this refers to a solvated film. The estimated dry thicknesses of the films (based on coulometry and monomer molar volume; see figure legends) are in the range 0.52–0.62 μm. No physically reasonable amount of roughness could be within an order of magnitude of the film-probe beam distance of 50–100 μm, so we discount surface roughness as a source of any optical artefact. We therefore consider factors associated with the DES, namely its optical and transport properties. Brief consideration of the refractive indices of the DES components shows that, while one would not anticipate large refractive index gradients, they would nonetheless be readily measurable under the experimental conditions; the observation of significant changes and excellent signal:noise (see Figs. 2 and 3 for representative data) supports this argument.

We are therefore left to consider solution transport processes. At this stage of the analysis, we do not have diffusion coefficient values for the choline cation or the glycol chloride complex anions. However, we can make reasonable estimates based on Walden's rule; we do not imply that this model, developed for dilute aqueous solutions, provides a detailed physical description of ionic liquids, but its broad characteristics suffice for initial diagnostic purposes. The viscosities of Ethaline and Propaline under the experimental conditions (*ca.* 20 °C) are *ca.* 40 cP and *ca.* 80 cP, respectively (*cf.* 0.8 cP for acetonitrile and 1 cP for water). Within the limitations of the

simplistic Walden's rule approach, one would anticipate that these *increases* in viscosity would result in proportionate *decreases* in diffusion coefficients, to *ca.* 1.4×10^{-7} cm^2 s^{-1} and 0.7×10^{-7} cm^2 s^{-1} (see below).

The role of the convolution process is to account for the temporal shift in the optical signal from its electrical and acoustic counterparts as a result of the spatial separations of the detection systems: the current and mass (*via* resonant frequency) are measured at the site of the electrochemical process but the optical response is measured at some distance from it. This distance is typically 50–100 μm, dependent on the experiment, but ultimately limited by the radius of the focal zone in front of the electrode (typically 30–50 μm). Using $x \sim \sqrt{(\pi Dt)}$ for the distance traversed in time t, we estimate that species expelled from the film into acetonitrile will reach the detection zone of the laser beam in *ca.* 1 s. Although there is clearly a time lag introduced by this, *i.e.* a phase shift between the electrical/gravimetric and optical responses, the probe beam will "see" the process within the experimental timeframe. As a result, the convolution algorithm generates physically reasonable outcomes, as found above (see Fig. 5).

The evolution of the mass flux profile in front of the electrode as measured by the beam deflection is characterised by the lateness and spreading of the initial signal at the electrode due to diffusion of species. In case of semi-infinite linear diffusion, the mass flux at distance x from the electrode $J(x, t)$ is related to its magnitude $J(t)$ at the electrode through a convolution operation (*) with a transfer function $F(x, t)$ featuring the diffusion [52]:

$$J(x,t) = J(t) * F(x,t) \quad \text{with} \quad F(x,t) = \frac{x}{2(\pi Dt)^{1/2}} \exp\left(-\frac{x^2}{4Dt}\right) \tag{2}$$

in which D is the diffusivity of the transported species. The same operation can be applied to any signal measured at the electrode (QCM for instance) in order to compare quantitatively with the current signal (proportional to the mass flux). The inputs to the analysis are the interfacial fluxes at the corresponding time values; the convolution algorithm then calculates the flux at a distance x, with $x/D^{1/2}$ as a fitted parameter.

For the same electrode-probe beam separation, the time delay in the DES media will be of the order of 50–100 s; even then, the full impact of the interfacial processes will not be seen. For all but the very slowest scan rates, the reality is that the potential sweep will have switched direction before measurable amounts of released species have reached the optical detection zone (or the solution depletion of species entering the film impacts on the composition in the optical zone). Physically, the instantaneous interfacial reaction and that which the optical detection "sees" at the same time are then taking place in opposite directions. Interpretationally, the convolution algorithm cannot accommodate this situation.

In principle, the solution would be to operate at slow scan rates. The challenges this generates are twofold. First, the resultant fluxes – and thence concentration gradients – are smaller, so signal:noise is compromised. Second, on the extended timescales required, stray convection processes and thermally generated optical effects are more problematical. The feasibility of this will be explored in a future study. Here, we change to a potentiostatic control function and follow the EQCM/PBD responses following application of a potential step.

3.2. Film responses to potentiostatic control function

3.2.1. Raw data and qualitative interpretation

Figs. 6–8 show the electrochemical (i), gravimetric (Δm) and optical (θ) responses to a film exposed to 0.1 M $LiClO_4/CH_3CN$, Ethaline and Propaline, respectively. In each case, the film was

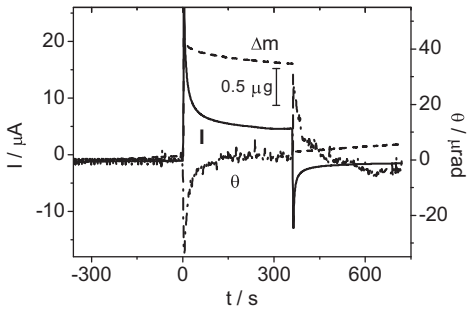

Fig. 6. Current (i; full line), mass (Δm; dashed line) and optical deflection (θ; dot-dashed line) responses to the application of a double potential step of a PEDOT film ($Q_{dep.}$ = 22.36 mC; dry thickness $h_f^0 = 0.52$ μm) exposed to 0.1 M $LiClO_4/CH_3CN$. After an initial equilibration period at −0.3 V, at t = 0 the potential was stepped from −0.3 V to 0.7 V; at t = 360 s the potential was returned to −0.3 V.

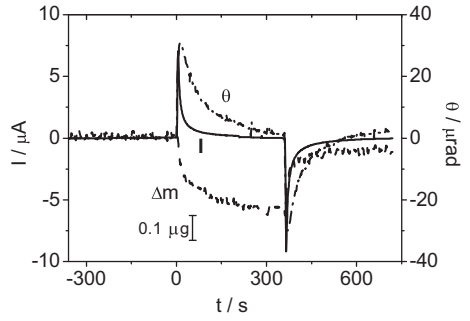

Fig. 7. Current (i; full line), mass (Δm; dashed line) and optical deflection (θ; dot-dashed line) responses to the application of a double potential step of a PEDOT film (as Fig. 6) exposed to Ethaline. After an initial equilibration period at −0.3 V, at t = 0 the potential was stepped from −0.3 V to 0.7 V; at t = 360 s the potential was returned to −0.3 V.

equilibrated in the reduced state (E = −0.3 V), oxidised (by a potential step to E = 0.7 V) and then reduced (by a potential step back to E = −0.3 V). Note that the "hold" period in each state, 360 s, exceeds that estimated to be the typical diffusion time even in the most viscous of the media (Propaline) by a factor of more than two.

In acetonitrile medium, there are strong *qualitative* similarities between the responses to a potential sweep (Fig. 1) and a potential step (Fig. 6). PEDOT oxidation is accompanied by a mass increase and a negative optical deflection; the reverse is the case upon subsequent film reduction. However, the observational timescales clearly have an effect. The gravimetric and optical responses are still changing at the potential reversal in the sweep experiment (Fig. 1): at the potential scan rate shown, this is only *ca.* 5 s after the peak potential

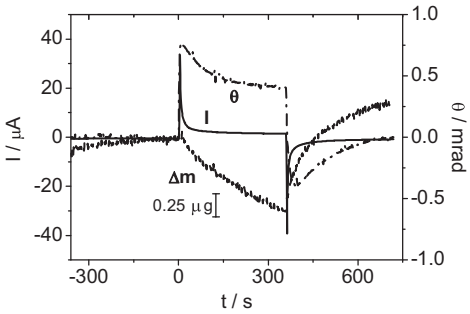

Fig. 8. Current (i; full line), mass (Δm; dashed line) and optical deflection (θ; dot-dashed line) responses to the application of a double potential step of a PEDOT film ($Q_{dep.}$ = 22.64 mC; dry thickness $h_f^0 = 0.52$ μm) exposed to Propaline. After an initial equilibration period at −0.3 V, at t = 0 the potential was stepped from −0.3 V to 0.7 V; at t = 360 s the potential was returned to −0.3 V.

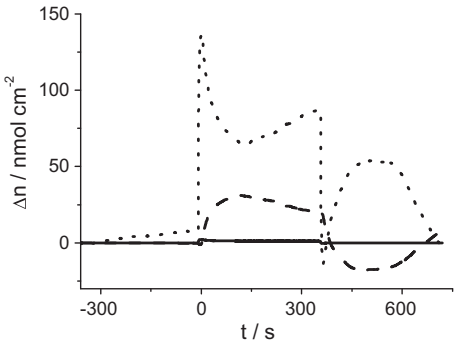

Fig. 9. Convolved data for double potential step experiment on a PEDOT film exposed to 0.1 M $LiClO_4/CH_3CN$; data from Fig. 6. Outcomes are expressed as time-dependent film population changes of cation (full line), anion (dashed line) and solvent (dotted line); all values referred to equilibrium populations at $E = -0.3$ V (for $t < 0$).

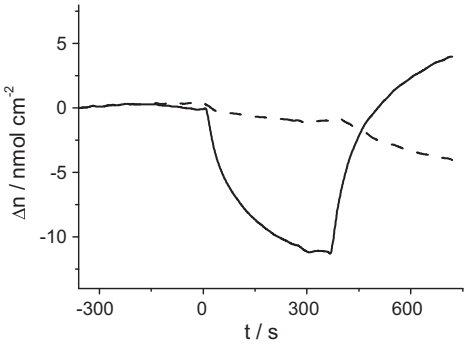

Fig. 11. Convolved data for double potential step experiment on a PEDOT film exposed to Propaline; data from Fig. 8. Outcomes are expressed as time-dependent film population changes of cation (full line) and anion (dashed line); all values referred to equilibrium populations at $E = -0.3$ V (for $t < 0$).

is passed. Inspection of the response to a potential step shows that changes are still taking place and being detected for *ca.* 100 s after the step.

In the two DES media (Figs. 7 and 8) the directional changes of the gravimetric and optical signals are opposite to their counterparts in acetonitrile solution; this is qualitatively consistent with the voltammetric data. The effect of observation on an extended timescale is similarly obvious, but with the additional feature that the PBD signal significantly lags the electrochemical and gravimetric signals. This is a consequence of the slow diffusional transport of species across the solution between the polymer/solution interface and the laser beam. It is worth noting that this delay is still significant, despite additional experimental effort being made in these particular measurements to position the laser beam closer to the surface, *i.e.* to minimise the diffusional transit time. The continuing presence of a compositional gradient in solution after *ca.* 200 s explains why it was not possible to convolve data from voltammetric experiments with timescales of the order of 50 s or less.

3.2.2. Quantitative interpretation

The outcomes of convolution of the chronoamperometric responses are shown in Figs. 9–11, expressed in terms of the film population changes of the mobile species. The $x/\sqrt{D}$ *vs* x plots (derived from convolution of identical electrochemical transients, but with the probe beam positioned at systematically varied distances from the surface), analogous to that shown in Fig. 5b for acetonitrile medium, gave diffusion coefficients of 1.1×10^{-6} cm^2 s^{-1} in Ethaline and 5.4×10^{-7} cm^2 s^{-1} in Propaline.

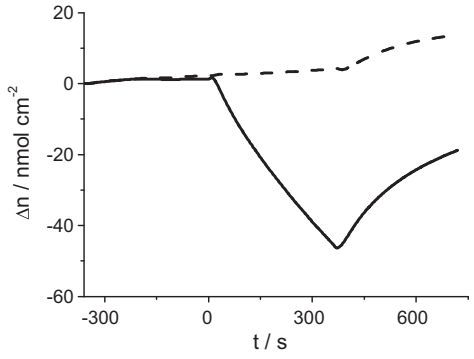

Fig. 10. Convolved data for double potential step experiment on a PEDOT film exposed to Ethaline; data from Fig. 7. Outcomes are expressed as time-dependent film population changes of cation (full line) and anion (dashed line); all values referred to equilibrium populations at $E = -0.3$ V (for $t < 0$).

While these values are not as small as the estimates based on simplistic application of Walden's rule (see above), they are clearly substantially below that for the diffusional transport process operative in acetonitrile. Their relative values (different by a factor of two) are consistent with the relative viscosities of Ethaline and Propaline. Most importantly, their values explain the difficulty in applying the convolution protocol to the voltammetric data (see above).

For PEDOT redox switching in acetonitrile (see Fig. 9), the primary observation is the dominance of anion transfer as the mechanism for maintaining electroneutrality; there is essentially no cation transfer (note that the full line representing cation population change is almost coincident with the x-axis). There is a significant amount of solvent transfer and the population changes are non-monotonic. While a sharp spike at very short times might be attributable to the discontinuity at that time (either in terms of the measured signal or the ability of the convolution protocol to deal with this), here the "spike" persists for a substantial period of time. We have no additional direct evidence to explain this, but we suggest that the difference from the response under voltammetric conditions may be a result of different compositional profiles within the film in the two cases. In the voltammetric case, particularly at low/moderate scan rates, there is adequate time for equilibration of mobile species populations within the film: under these conditions, the film is compositionally homogeneous. However, immediately after the application of a potential step, film composition (notably solvation) will be non-homogeneous and on longer timescales there will be a need to restore homogeneity and equilibrium, which might for example require expulsion of excess solvent. Additionally, we note that there appear to be longer term changes in the anion population. We are hesitant to interpret these in detail for the following reasons. The success of the convolution protocol for voltammetric experiments in acetonitrile is attributable to the fact that most of the processes in the film and particularly in the solution are relatively rapid; the (electro)chemical information is available relatively promptly. After several hundred seconds (as in the later stages of the chronoamperometric experiments) the current response decreases to background levels, *i.e.* there will be little Faradaic response for the system to report. However, even relatively small background currents, when integrated over substantial times and interpreted Faradaically, can give the impression of significant population change; to put this in context, a background current of 2.5 μA (at the electrodes used) over a period of 100 s would correspond to a population change of *ca.* 10 nmol cm^{-2}. In summary, the very feature that makes the acetonitrile data tractable on short timescales is that which makes it vulnerable to background current

on long timescales. We therefore do not place emphasis on the long timescale response in this medium.

Turning to the more interesting and, from the perspective of the earlier part of this study, problematical cases of PEDOT redox switching in the DES media, the outcomes are both simpler and clearer. The responses in Figs. 10 and 11 show the dominance of cation transfer, as was the deduced *qualitatively* under voltammetric conditions. The timescale of the changes (several hundred seconds) demonstrates why the voltammetric data could not be interpreted using the convolution protocol. From a methodological perspective, the convolution analysis returns a "net neutral" species population change. The interpretation of this for the DES media is subtly different to that in acetonitrile (for which "net neutral" species is synonymous with "solvent"). In the DES media, "net neutral" species corresponds to anions and cations in charge balanced amounts, which can be partitioned into cation and anion transfers that can in turn be summed with the separately determined ion transfers from the convolution process. Thus, there is no neutral species trace in Figs. 10 and 11.

One of the initial objectives of the study was to determine whether there was a substantive reservoir of electrolyte in the films, adequate to provide a source of cations for expulsion throughout the oxidation process. The data of Figs. 10 and 11 clearly indicate that this is indeed the case. This contrasts sharply with the $LiClO_4/CH_3CN$ case, where there was no evidence of any film-based cation reservoir.

4. Conclusions

A combined EQCM/PBD approach has been used to explore mechanistic aspects (ion and solvent transfers) of the redox switching of PEDOT films in a molecular electrolyte system (acetonitrile) and two deep eutectic solvent media (Ethaline 200 and Propaline 200). In overview, the electrochemical response (current) yields the electron flux across the *electrode/polymer interface*, the acoustic response (mass change) provides changes in film composition *via* transfers at the *polymer/solution interface* and the optical response (beam deflection) contains information about transport of the species ejected from the film (or injected into it) as they traverse the solution from the polymer to the optical beam (or from the optical beam to the polymer).

When a potentiodynamic control function is used, peak current values in all three media are linear with scan rate and have very similar values. The magnitude of the overall mass change in each electrolyte is essentially independent of scan rate (timescale), but quite different in the three media. This indicates complete redox conversion, but by different mechanisms and using different sources/sinks of mobile species in each case. The accompanying optical deflection data depend markedly on solution composition. In acetonitrile, the optical signal excursion varies with the square root of scan rate, suggesting a diffusional process. In the DES media, the magnitude of the signal initially increases with scan rate, then decreases.

For PEDOT exposed to $LiClO_4/CH_3CN$, the EQCM/PBD responses are amenable to the convolution protocol, permitting the electrochemical, gravimetric and optical signals to be correlated. The outcome of this analysis is dominance of electroneutrality maintenance by anion transfer (permselectivity), with accompanying transfer of some solvent. In the deep eutectic solvents, the mass and optical deflection responses are in the opposite directions to their counterparts in acetonitrile, suggesting a cation transfer-based mechanism; there is no molecular solvent to be considered. Convolution of voltammetric responses in the DES media was not possible. This is attributable to the long transit times in these viscous media of mobile species from the polymer/solution interface to the optical detection zone, as signalled by the decrease in optical signal with increasing scan rate (decreasing observational time).

The delayed optical response in the very viscous DES media can be overcome by the use of an extended observational timescale, here developed in the context of a chronoamperometric experiment. In acetonitrile medium, there are strong *qualitative* similarities between the responses to a potential sweep and a potential step, although the different potential profiles and observational timescales do have an effect on the *quantitative* temporal population changes. Convolution of the chronoamperometric responses in the DES media is possible under these conditions and reveals film population changes on extended timescales. Solution transport is characterised by diffusion coefficients an order of magnitude (or more) smaller than in acetonitrile. In both DES media used, the primary observation is dominance of cation transfer, as was deduced *qualitatively* under voltammetric conditions. There is clearly a substantive reservoir of electrolyte in the films, adequate to provide a source of cations for expulsion throughout the oxidation process. This contrasts sharply with the $LiClO_4/CH_3CN$ case, where there was no evidence of any film-based cation reservoir.

This study represents the first application of the combined EQCM/PBD methodology to deep eutectic solvents. The facility of the methodology to explore in a systematic manner the processes occurring at the various interfaces and in the solution within a single experiment is extremely powerful and should find wider applicability in the development of these novel media for a range of practical applications.

Acknowledgement

We thank Gamry for support in terms of instrumentation. V.C. Ferreira gratefully acknowledges FCT for financial support (SFRH/BPD/77404/2011).

References

[1] T.A. Skotheim (Ed.), Handbook of Conducting Polymers, 2nd edn., Marcel Dekker, New York, 1998.
[2] P. Chandrasekhar, Conducting Polymers, Fundamentals and Applications. A Practical Approach, Kluwer Academic Publishers, Boston, 1999.
[3] H.R. Jung, W.J. Lee, Ag/poly(3,4-ethylenedioxythiophene) nanocomposites as anode materials for lithium ion battery, Solid State Ionics 187 (2011) 50.
[4] A. Luzio, C. Musumeci, C.R. Newman, A. Facchetti, T.J. Marks, B. Pignataro, Enhanced Thin-Film Transistor Performance by Combining 13,6-NSulfinylacetamidopentacene with Printed PEDOT:PSS Electrodes, Chem. Mater. 23 (2011) 1061.
[5] M. Knoll, M. Thamer, An enhancement-mode electrochemical organic field-effect transistor, Electrochem. Commun. 13 (2011) 597.
[6] R.M.G. Rajapakse, S.J. Higgins, K. Velauthamurty, H.M.N. Bandara, S. Wijeratne, R.M.M.Y. Rajapakse, Nanocomposites of poly(3,4-ethylenedioxythiophene) and montmorillonite clay: synthesis and characterization, J. Compos. Mater. 45 (2011) 597.
[7] Y.J. Xia, H.M. Zhang, J.Y. Ouyang, Highly conductive PEDOT: PSS films prepared through a treatment with zwitterions and their application in polymer photovoltaic cells, J. Mater. Chem. 20 (2010) 9740.
[8] P.C. Barbosa, L.C. Rodrigues, M.M. Silva, M.J. Smith, A.J. Parola, F. Pina, C. Pinheiro, Solid-state electrochromic devices using pTMC/PEO blends as polymer electrolytes, Electrochim. Acta 55 (2010) 1495.
[9] S. Liu, L. Xu, F. Li, B. Xu, Z. Sun, Enhanced electrochromic performance of composite films by combination of polyoxometalate with poly(3,4-ethylenedioxythiophene), J. Mater. Chem. 21 (2011) 1946.
[10] L. Adamczyk, P.J. Kulesza, Fabrication of composite coatings of 4-(pyrrole-1-yl) benzoate-modified poly-3,4-ethylenedioxythiophene with phosphomolybdate and their application in corrosion protection, Electrochim. Acta 56 (2011) 3649.
[11] J.A. Chikar, J.L. Hendricks, S.M. Richardson-Burns, Y. Raphael, B.E. Pfingst, D.C. Martin, The use of a dual PEDOT and RGD-functionalized alginate hydrogel coating to provide sustained drug delivery and improved cochlear implant function, Biomaterials 33 (2012) 1982.
[12] J.A. Arter, J.E. Diaz, K.C. Donavan, T. Yuan, R.M. Penner, G.A. Weiss, Virus-polymer hybrid nanowires tailored to detect prostate-specific membrane antigen, Anal. Chem. 84 (2012) 2776.
[13] M. Ilieva, V. Tsakova, W. Erfurth, Electrochemical formation of bi-metal (copper–palladium) electrocatalyst supported on poly-3,4-ethylenedioxythiophene, Electrochim. Acta 52 (2006) 816.

[14] J.A. Avila-Nino, E. Segura-Cardenas, A.O. Sustaita, I. Cruz-Cruz, R. Lopez-Sandoval, M. Reyes-Reyes, Nonvolatile write-once-read-many-times memory device with functionalized-nanoshells/PEDOT: PSS nanocomposites, Mater. Sci. Eng. B 176 (2011) 462.
[15] V.A. Lifton, S. Simon, Preparation and electrowetting transitions on super-hydrophobic/hydrophilic bi-layer structures, J. Porous Mater. 18 (2011) 535.
[16] K. Ikushima, S. John, A. Ono, S. Nagamitsu, PEDOT/PSS bending actuators for autofocus micro lens applications, Synth. Met. 160 (2010) 1877.
[17] J. Bobacka, A. Lewenstam, A. Ivaska, Electrochemical impedance spectroscopy of oxidized poly(3,4-ethylenedioxythiophene) film electrodes in aqueous solutions, J. Electroanal. Chem. 489 (2000) 17.
[18] H. Randriamahazaka, C. Plesse, D. Teyssie, C. Chevrot, Electrochemical behaviour of poly(3,4-ethylenedioxythiophene) in a room-temperature ionic liquid, Electrochem. Commun. 5 (2003) 613.
[19] C. Li, T. Imae, Electrochemical and optical properties of the poly(3,4-ethylenedioxythiophene) film electropolymerized in an aqueous sodium dodecyl sulfate and lithium tetrafluoroborate medium, Macromolecules 37 (2004) 2411.
[20] A. Bund, S. Neudeck, Effect of the solvent and the anion on the doping/dedoping behavior of poly(3,4-ethylenedioxythiophene) films studied with the electrochemical quartz microbalance, J. Phys. Chem. B 108 (2004) 17845.
[21] A.R. Hillman, S.J. Daisley, S. Bruckenstein, Kinetics and mechanism of the electrochemical p-doping of PEDOT, Electrochem. Commun. 9 (2007) 1316.
[22] A.R. Hillman, S.J. Daisley, S. Bruckenstein, Ion and solvent transfers and trapping phenomena during n-doping of PEDOT films, Electrochim. Acta 53 (2008) 3763.
[23] B. Ulgut, J.E. Grose, Y. Kiya, D.C. Ralph, H.D. Abruna, A new interpretation of electrochemical impedance spectroscopy to measure accurate doping levels for conducting polymers: Separating Faradaic and capacitive currents, J. Appl. Surf. Sci. 256 (2009) 1304.
[24] H. Randriamahazaka, T. Bonnotte, V. Noel, P. Martin, J. Ghilane, K. Asaka, J.C. Lacroix, Medium effects on the nucleation and growth mechanisms during the redox switching dynamics of conducting polymers: case of poly(3,4-ethylenedioxythiophene), J. Phys. Chem. B 115 (2011) 205.
[25] M.A. Skopek, M.A. Mohamoud, K.S. Ryder, A.R. Hillman, Nanogravimetric observation of unexpected ion exchange characteristics for polypyrrole film p-doping in a deep eutectic ionic liquid, Chem. Commun. (2009) 935.
[26] N. Levy, M.D. Levi, D. Aurbach, R. Demadrille, A. Pron, Failure and stabilization mechanisms in multiply cycled conducting polymers for energy storage devices, J. Phys. Chem. C 114 (2010) 16823.
[27] Q. Hao, W. Lei, X. Xia, Z. Yan, X. Yang, L. Lu, X. Wang, Exchange of counter anions in electropolymerized polyaniline films, Electrochim. Acta 55 (2010) 632.
[28] A. Rubin, H. Perrot, C. Gabrielli, M.C. Pham, B. Piro, Electrochemical and electrogravimetric behaviors of conducting polymer. Theoretical aspects and application to co-polymer films based on juglone, Electrochim. Acta 55 (2010) 6136.
[29] A.R. Hillman, S. Bruckenstein, Role of film history and observational timescale on redox switching kinetics of electroactive films. Part 1. - A new model for permselective films with polymer relaxation processes, Faraday Trans. 89 (1993) 339.
[30] A.R. Hillman, S. Bruckenstein, Role of film history and observational timescale in redox switching kinetics of electroactive films. Part 2. - Visualizing electrochemical redox switching pathways involving four or more distinct relaxation times, Faraday Trans. 89 (1993) 3779.
[31] A.R. Hillman, I. Efimov, K.S. Ryder, Time-scale- and temperature-dependent mechanical properties of viscoelastic poly(3,4-ethylenedioxythiophene) films, J. Am. Chem. Soc. 127 (2005) 16611.
[32] A.R. Hillman, M.A. Mohamoud, I. Efimov, Time-temperature superposition and the controlling role of solvation in the viscoelastic properties of polyaniline thin films, Anal. Chem. 83 (2011) 5696.
[33] C.M. Amb, A.L. Dyer, J.R. Reynolds, Navigating the color palette of solution-processable electrochromic polymers, Chem. Mater. 23 (2011) 397.
[34] T.A. Skotheim, J.R. Reynolds (Eds.), Handbook of Conducting Polymers: Processing and Applications, 3rd edn., CRC Press, Boca Raton, 2007.
[35] R.R. Sondergaard, M. Hosel, F.C. Krebs, Roll–to–Roll fabrication of large area functional organic materials, J. Polym. Sci. B 51 (2013) 16.
[36] T. Yang, H. Wang, X.M. Ou, C.S. Lee, X.H. Zhang, Iodine-doped-poly(3,4-ethylenedioxythiophene)-modified Si nanowire 1D core-shell arrays as an efficient photocatalyst for solar hydrogen generation, Adv. Mater. 24 (2012) 6199.
[37] K. Opwis, D. Knittel, J.S. Gutmann, Oxidative in situ deposition of conductive PEDOT:PTSA on textile substrates and their application as textile heating element, Synth. Met. 162 (2012) 1912.
[38] S. Tuukkanen, T. Julin, V. Rantanen, M. Zakrzewski, P. Moilanen, K.E. Lilja, S. Rajala, Solution-processible electrode materials for a heat-sensitive piezoelectric thin-film sensor, Synth. Met. 162 (2012) 1987.
[39] Z. Tang, Z. George, Z.F. Ma, J. Bergqvist, K. Tvingstedt, K. Vandewal, E. Wang, L.M. Andersson, M.R. Andersson, F.L. Zhang, O. Inganas, Semi-transparent tandem organic solar cells with 90% internal quantum efficiency, Adv. Energ. Mater. 2 (2012) 1467.
[40] P. Morvillo, I.A. Grimaldi, R. Diana, F. Loffredo, F. Villani, Study of the microstructure of inkjet-printed P_3HT:PCBM blend for photovoltaic applications, J. Mater. Sci. 48 (2013) 2920.
[41] A.P. Abbott, K.J. McKenzie, Application of ionic liquids to the electrodeposition of metals, Phys. Chem. Chem. Phys. 8 (2006) 4265.
[42] D.R. MacFarlane, J.M. Pringle, P.C. Howlett, M. Forsyth, Ionic liquids and reactions at the electrochemical interface, Phys. Chem. Chem. Phys. 12 (2010) 1659.
[43] S. Fletcher, V.J. Black, I. Kirkpatrick, T.S. Varley, Quantum design of ionic liquids for extreme chemical inertness and a new theory of the glass transition, J. Solid State Electrochem. 17 (2013) 327.
[44] M. Figueiredo, C. Gomes, R. Costa, A. Martins, C.M. Pereira, F. Silva, Differential capacity of a deep eutectic solvent based on choline chloride and glycerol on solid electrodes, Electrochim. Acta 54 (2009) 2630.
[45] A.P. Abbott, G. Frisch, S.J. Gurman, A.R. Hillman, J. Hartley, F. Holyoak, K.S. Ryder, Ionometallurgy: designer redox properties for metal processing, Chem. Commun. 47 (2011) 10031.
[46] A.R. Hillman, K.S. Ryder, C.J. Zaleski, C. Fullarton, E.L. Smith, Ion transfer mechanisms accompanying p-doping of poly(3,4-ethylenedioxythiophene) films in deep eutectic solvents, Z. Phys. Chem. 226 (2012) 1049.
[47] S. Bruckenstein, A.R. Hillman, Consequences of thermodynamic restraints on solvent and ion transfer during redox switching of electroactive polymers, J. Phys. Chem. 92 (1988) 4837.
[48] S. Bruckenstein, A.R. Hillman, Solvent and salt transfer upon redox switching of electroactive polymers, J. Phys. Chem. 95 (1991) 10748.
[49] M.J. Henderson, H. French, A.R. Hillman, E. Vieil, A combined EQCM and probe beam deflection study of salicylate ion transfer at a polypyrrole modified electrode, Electrochem, Solid State Lett. 2 (1999) 631.
[50] M.J. Henderson, A.R. Hillman, E. Vieil, Chronoamperometric resolution of ion and solvent transfers at a poly(o-toluidine) modified electrode by combined electrochemical quartz crystal microbalance (EQCM) and probe beam deflection (PBD), Electrochim. Acta 45 (2000) 3885.
[51] C. Barbero, Ion exchange at the electrode/electrolyte interface studied by probe beam deflection techniques, Phys. Chem. Chem. Phys. 7 (2005) 1885.
[52] E. Vieil, Mass transfer and convolution. Part 1. Theory, J. Electroanal. Chem. 264 (1994) 9.
[53] A.P. Abbott, S. Nandhra, S. Postlethwaite, E.L. Smith, Electroless deposition of metallic silver from a choline chloride-based ionic liquid: a study using acoustic impedance spectroscopy, SEM and atomic force microscopy, Phys. Chem. Chem. Phys. 9 (2007) 3735.
[54] G. Sauerbrey, Verwendung von Schwingquarzen zur Wägung dünner Schichten und zur Mikrowägung, Z. Phys. 155 (1959) 206.